Colloid and Polymer Science (2021) 299:1357–1369
https://doi.org/10.1007/s00396-021-04846-1

ORIGINAL CONTRIBUTION

One-pot synthesis of double and triple polybetaine block copolymers and their temperature-responsive solution behavior

Jongmin Lim[1] · Hideki Matsuoka[1] · Yoshiyuki Saruwatari[2]

Received: 2 February 2021 / Revised: 21 April 2021 / Accepted: 6 May 2021 / Published online: 17 June 2021

Abstract

Di- and triblock betaine copolymers composed of a sulfobetaine with a carboxy/phosphobetaine were synthesized by one-pot aqueous reversible addition-fragmentation chain transfer (RAFT) polymerization. The betaine methacrylate monomers were fully converted at each step by tuning the concentrations of the monomers, the chain transfer agent, and the initiator. AB-type diblocks poly(carboxybetaine methacrylate)-*b*-poly(sulfobetaine methacrylate) (PGLBT-*b*-PSPE) and poly(2-(methacryloyloxy)ethyl phosphorylcholine)-*b*-poly(sulfobetaine methacrylate) (PMPC-*b*-PSPE) were prepared to have identical unit numbers with different total molecular weights. Unlike homo-polysulfobetaine solutions or PGLBT-*b*-PSPEs in our previous report, the aqueous solutions of those diblock copolymers showed weak upper critical solution temperature (UCST) behavior, monitored by transmittance/dynamic light scattering. Even at the lowest temperature, the diblock chains remained in the unimer/aggregate polydisperse state, which is the intermediate stage prior to the emergence of monodisperse micelles. It is thought that the UCST behavior that originated from electrostatic attraction among PSPE motifs was interfered by temperature-inert motifs (PGLBT/PMPC) on the opposite side, having nearly the same unit number. The BAB-type triblock copolymer PSPE-*b*-PGLBT-*b*-PSPE with a 1:1:1 stoichiometry showed a clearer transmittance shift and size variation due to the increased ratio of PSPE at both chain ends. While the transmittance gradually decreased by cooling, larger aggregates (~ 700 nm) than those of diblocks (~ 180 nm) emerged with unimers. The small-large diffusive modes transformed into a monodisperse mode at much lower temperatures, which is assumed to be flower-like micelles consisting of PGLBT-loop coronas and PSPE core. However, another sample of 1:2:1 stoichiometry showed incomplete transition as diblocks having a similar AB ratio.

Keywords Polybetaines · Double hydrophilic block copolymers · Temperature-responsive polymers · Polymer self-assembly · Aqueous RAFT polymerization

Introduction

Studies on polyzwitterions and their derivative copolymers have been extensively carried out to utilize their unique characteristics. Having ionic groups with opposite signs on the same repeating unit, the overall charge of polyzwitterions is inherently neutral and exhibits distinguished properties from polyelectrolytes and non-ionic polymers [1]. Ionic polymers usually associate with counterions to keep neutrality and collapse by salt addition ("salting-out" behavior), which is attributed to reduced net charge and hydrophilicity. However, polyzwitterions which basically do not contain counterions attract or repel each other between their charged functional groups, and become more soluble and swell in water under increasing salt ("salting-in" behavior). Dipole–dipole interactions between oppositely charged groups in other chains or the same chain make them globulized and may result in aggregations in salt-free water, and addition of low molecular weight salts hinders those pairings by charge screening [2]. Among several kinds of polyzwitterions, polysulfobetaines are particularly known for upper critical solution temperature (UCST) behavior in aqueous solution because of strong electrostatic attraction. The critical temperature of polysulfobetaine aqueous solutions is also under the influence of salt presence: a larger amount of salts retards the

✉ Hideki Matsuoka
matsuoka.hideki.3s@kyoto-u.ac.jp

[1] Department of Polymer Chemistry, Kyoto University, Katsura, Nishikyo-ku, Kyoto 615-8510, Japan

[2] Osaka Organic Chemical Industry Ltd, 7-20 Azuchi-machi, 1chome, Chuo-ku, Osaka 541-0052, Japan

phase separation to lower temperatures by charge screening [3, 4]. The dipole orientation among polyzwitterion chains is captured as slow diffusive modes simultaneously appearing with fast-diffusing modes representing unimers in dynamic light scattering study [5–8], which seem to be analogous to "ordinary–extraordinary" transition observed in polyelectrolytes solutions [9–11] but may be brought by different mechanisms.

Besides, polyzwitterions have a distinctive hydration layer as representing an "unperturbed" state according to the studies observing hydrogen bonding around zwitterionic units using Raman [12, 13] or sum frequency generation (SFG) vibrational spectroscopy [14, 15]. Hydrogen bonding (H-bonding) of water molecules at the vicinity of zwitterionic units are not disrupted and the ordering does not have significant differences from that in bulk water, contrary to typical polyelectrolytes causing disruption of H-bonding [16]. Thanks to the unperturbed state of H-bonding and tightly bound water molecules on the chain surface, polyzwitterions generally show remarkable nonfouling behavior. Replacement of water molecules around polyzwitterions to other molecules which can adsorb on the surface was more difficult than at non-ionic poly(ethylene glycol) (PEG) or oligo(ethylene glycol) methacrylate (OEGMA) chains [14]. Polyzwitterion-coated 2D surfaces were evaluated to have superior antifouling property than OEGMA or self-assembled monolayers [17] and polyelectrolyte surface [18] on protein adsorption.

The traits have been utilized by copolymerizing zwitterionic monomers with other non-ionic hydrophilic/hydrophobic units to modify and add properties. Random copolymers consisting of non-ionic [19–22], ionic units [23], or different kinds of zwitterionic monomers [24, 25] were tested. Polybetaine-based amphiphilic [26–29], double hydrophilic [30, 31], and dual stimulus–responsive [32–36] block copolymers were also developed. Previously, we synthesized a double hydrophilic betaine block copolymer PGLBT-*b*-PSPE (2-((2-(methacryloyloxy)ethyl)dimethylammonio)acetate-*b*-3-((2-(methacryloyloxy)ethyl)dimethylammonio)propane-1-sulfonate) by reversible addition-fragmentation chain transfer (RAFT) polymerization and elucidated their responses to temperature, pH, and salts in aqueous media [37–39]. PSPE segments became gradually hydrophobic relative to the opposite side by temperature decrease, then the increased difference of water affinity led to self-assembled structures whose inner side is mostly PSPE to minimize enthalpic penalty under the critical temperature. A recent small-angle X-ray (SAXS) study of carboxy-sulfobetaine block copolymer concentrated aqueous solutions showed a lyotropic morphology transition driven by the selective hydration of carboxybetaine segments [40]. However, the ratio of PGLBT and PSPE was only roughly controllable because of the low percentage of macroCTA chains (PGLBT homopolymers) properly functioned in the second polymerization step by indiscernible reasons, presumably related to the stability of the RAFT functional groups. For that reason, the effect of block ratio and total repeating unit numbers on the characteristics of PGLBT-*b*-PSPE was not elucidated in detail. An ABA triblock copolymer of PSPE (a) and phosphobetaine methacrylate (b) was synthesized by two-step electron transfer atom transfer radical polymerization (ARGET ATRP) with a bifunctional initiator, and demonstrated a characteristic behavior in aqueous solutions and an ionic liquid attributed to the zwitterionic functional groups [41]. However, thorough removal of catalysts for each step was needed.

In this study, we performed one-pot synthesis of betaine methacrylate-based diblock and triblock copolymers by applying the methodology extensively investigated by Perrier's group [42–46] to avoid factors which may destabilize RAFT functionality, and to obtain well-defined block copolymers through a more accessible process within less preparation time.

Experimental section

Materials

2-((2-(Methacryloyloxy)ethyl)dimethylammonio)acetate (carboxybetaine methacrylate, GLBT) and 3-((2-(methacryloyloxy)ethyl)dimethylammonio)propane-1-sulfonate (sulfobetaine methacrylate, SPE, also referred to SBMA in other reports) were kindly donated from Osaka Organic Chemical Industry LTD (Osaka, Japan) and used as received. 2-Methacryloyloxyethyl phosphorylcholine (MPC) was a kind donation from K. Ishihara's group (Univ. of Tokyo). 4-Cyano-4-(2-phenylethanesulfanylthiocarbonyl)sulfanylpentanoic acid (PETTC) was synthesized according to the literature[47] and used as a chain transfer agent (CTA). The radical initiator 2,2′-azobis[2-(2-imidazolin-2-yl)propane]dihydrochloride (VA-044, 97%, Wako) and 2,2,2-trifluoroethanol (TFE, 99%, Nacalai Tesque) were used as received. Deuterated water (D_2O) was purchased from Cambridge Isotope Laboratories. Ultrapure water (minimum resistivity ~ 18.2 MΩ cm) obtained by the Milli-Q system was used for synthesis, dialysis, and aqueous solution sample preparation. Dialysis was performed using regenerated cellulose membranes (MWCO 3500 and 15,000) to remove residues.

Block copolymer synthesis by consecutive RAFT polymerization

Firstly, CTA (PETTC), monomer, initiator, water, and TFE (8:2, v/v) were put into a rubber septum-sealed glass vial with a magnetic stirrer. After vigorous mixing and degassing by 15 min of argon bubbling, the vial was placed in an oil bath thermostated at 70 °C to start RAFT polymerization.

Aliquots were taken during synthesis using a syringe for ^{1}H NMR and SEC analysis. Once full monomer consumption was confirmed, the vial was transferred in an ice bath and cooled to end the reaction. For additional blocks, new monomers were added to the vial with additional initiator and water, and the reactant solution was degassed before the initiation of the next polymerization. The procedure was repeated until the target block copolymers were obtained. The final products were purified by dialysis against Milli-Q water. The reservoir was discarded twice per day until the electric conductivity of reservoir water was equlibrated then lyophilized to yield yellow powder. The detailed experimental conditions are shown in Scheme 1 and Tables S1–S3.

Polymer characterization

^{1}H nuclear magnetic resonance (NMR) spectra of synthesized polymers were acquired on a 400 MHz JEOL JNM-AL400 spectrometer (JEOL, Tokyo, Japan) in deuterated water (D_2O). Chemical shifts (δ) are reported in ppm relative to H_2O (4.75 ppm). Minimum 64 scans were recorded for each sample.

Aqueous size exclusion chromatography (SEC) was performed with a column (SB-804 HQ, Shodex) and a refractive index detector (RI-830, JASCO, Japan), using a buffer eluent (0.5 M CH_3COOH and 0.3 M of Na_2SO_4) at a flow rate of 0.5 mL/min. The number-average molecular weight (M_n) and dispersity (M_w/M_n, denoted as $Đ$) of each homo- and multiblock copolymers were determined by the calibration performed with a set of poly(2-vinylpyridine) standards. (M_n range 5500 to 142,000 g/mol, Sigma-Aldrich).

The transmittance at 200–600 nm for the aqueous solutions of the block copolymers were recorded from 60 to ~ 5 °C at regular intervals after waiting for 5 min at each temperature using a UV-VIS spectrometer (Hitachi U-3310 spectrophotometer) equipped with a temperature-controlling water circulator. A quartz cell with a light path of 10 mm was used. Each solution was filtered by a syringe filter unit (pore size 0.2 µm, mdi) prior to measurement. The transmittance value at 400 nm was taken for the plot against temperature.

Dynamic light scattering (DLS) was performed to measure the hydrodynamic radius (R_h) of the polymers in aqueous solution. A goniometer (BI-200SM, Brookhaven Instruments, New York, USA) equipped with a 15-mW He–Ne laser (wavelength $\lambda = 632.8$ nm) and a water circulator was used. (index matching fluid = decahydronaphthalene). The field autocorrelation functions were obtained by a BI-DS2 photomultiplier tube with a correlator (TurboCorr, Brookhaven Instruments) at four scattering angles (60°, 75°, 90°, and 105°) and analyzed by CONTIN regularization. All the autocorrelation functions (ACFs) are reported as $((g^{(2)}(q,t)-1)/\beta)^{0.5}$. The details of light scattering are described in the supporting information page. The concentration of polymer aqueous solution samples of transmittance and DLS measurement was 10 mg/mL.

Determination of monomer conversions

The monomer conversions were calculated from ^{1}H NMR spectra using the following equation as described in the literature [45]:

$$p = \frac{[M]_0 - [M]_t}{[M]_0} = 1 - \frac{[M]_t}{[M]_0} = 1 - \frac{\frac{\int I_{5.7-6.2ppm}}{\int I_{CTA}}}{DP_{target}} \quad (1)$$

where $[M]_0$ and $[M]_t$ are the monomer concentrations at the initial and passed time t, and $\int I_{5.7-6.2\ ppm} / \int I_{CTA}$ is the corrected proton ratio of the unreacted monomer to the CTA at the end of the chain. DP_{target} is the targeted number-average degree of polymerization. Each conversion was also determined by the following equation:

$$p = \frac{\int I_p}{\int I_p + \int I_m} \quad (2)$$

where $\int I_p$ is the corrected integral value of polymer peaks and $\int I_m$ is that for vinyl protons of the monomer.

Determination of number-average theoretical molecular weight ($M_{n,\ theo}$) and theoretical living chain fraction

By the following equation introduced in the work of Gody et al. [42], $M_{n,theo}$ can be determined as the following equation:

$$M_{n,\ theo} = \frac{[M]_0 \bullet p \bullet M_M}{[CTA]_0 + 2f[I]_0(1 - e^{-k_d t})(1 - \frac{f_c}{2})} + M_{CTA} \approx p \bullet DP_{target} \bullet M_M + M_{CTA} \quad (3)$$

where $[M]_0$, $[CTA]_0$, and $[I]_0$ are the initial concentration of monomer, CTA, and initiator, respectively. M_M and M_{CTA} are the molar mass of the monomer and CTA, respectively. k_d is the decomposition rate constant of the azoinitiator. ($k_{d(VA-044,70°C)} = 4.2995 \times 10^{-4} s^{-1}$, which was an estimated value in the literature [42]). t is the time of polymerization. The term $2f$ means that one azoinitiator molecule provides two radicals with the efficiency f. (f was set to 0.5 in the study.) The coupling factor f_c represents the ratio of chain termination types. ($f_c = 1$ is combination of two active chain ends and $f_c = 0$ is radical disproportionation.) In this study, the initiator term could be dismissed as 0 due to the negligible amount of the participated initiator, so the equation can

be reduced as the form of the right side. Following the same concept [42], the theoretical livingness of chains (% of CTA-ended chains) could be expressed by the Eq. (4):

$$L = \frac{[CTA]_0}{[CTA]_0 + 2f[I]_0(1 - e^{-k_d t})(1 - \frac{f_c}{2})} \quad (4)$$

Results and discussions

In our previous report [37], the carboxybetaine-sulfobetaine diblock copolymer PGLBT-*b*-PSPE was synthesized by RAFT polymerization following conventional procedures for block copolymerization. PGLBT homopolymers were synthesized using a dithobenzoate type RAFT agent (4-cyanopentanoic acid dithiobenzoate) (CPADB), which is widely used as water-soluble CTA for methacrylate monomers. Unlike synthesis of polybetaine derivative block copolymers that consist of hydrophobic or anionic/cationic units or even a random betaine copolymer (PGLBT-*r*-PSPE), the activity of macroCTA (homo-PGLBT) was severely lost in the second polymerization step. Only a few PGLBT homopolymers were involved in PSPE growth, and resulted in uncontrollable block ratios. Therefore, the removal of unreacted PGLBT by precipitation into methanol was necessitated. Hydrolytic cleavage of the dithiobenzoate end group was assumed to occur when they were exposed to water molecules [48], although the polymerization was conducted at a lowered temperature (45 °C) by using a faster decomposing azoinitiator (VA-044) to prevent possible hydrolysis. Cyano-hydrolysis on the R group during usage or storage by water contamination [49] also could be the reason. Since trithiocarbonate-type RAFT agents are known for enhanced stability against hydrolysis and less retardation dependent on the concentration of CTA [50], we selected PETTC, which successfully conducted polymerization-induced self-assembly of amphiphilic methacrylate copolymers [47, 51–53]. Also, purification through dialysis prior to subsequent polymerization steps can be omitted by achieving full conversion of the monomers.

One-pot polymerization of PGLBT-*b*-PSPE and PMPC-*b*-PSPE

We aimed to produce PGLBT-*b*-PSPE having an identical block length as a model study. The targeted DP of each block was set to over 50 to make the block copolymers show temperature-responsive characters in an easily detectable temperature range. Typically, PSPE homopolymers obtained in our group whose target DP was 50–200 showed cloud points at 10–30 °C. PGLBT was synthesized prior to PSPE in order to remove possible homo-PGLBT residues in the final product created by incomplete conversion. The reactant solution containing GLBT, PETTC, and VA-044 in water/TFE mixture was placed in an oil bath thermostated at 70 °C (Scheme 1). Compared to the previous study, the temperature was increased from 45 to 70 °C to attain full conversion within a short reaction time by increasing the radical decomposition rate. Water was used as the main solvent because it is one of few good solvents for polybetaines. Moreover, it was reported to induce the highest propagation rate of acrylamide monomers [54]; hence, it is thought to

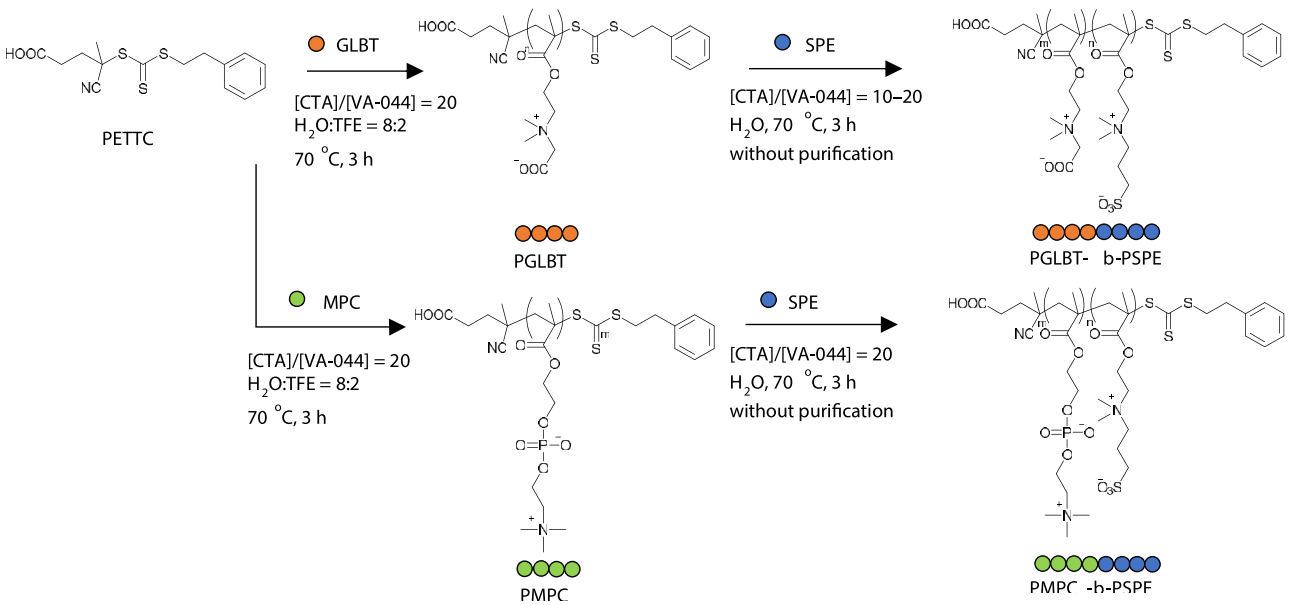

Scheme 1 Synthetic routes for the preparation of betaine diblock copolymers by one-pot RAFT polymerization

affect polymerization of methacrylates in the similar way. At the first polymerization step, TFE was required to compensate poor solubility of PETTC in water. Since only highly polar solvents with strong hydrogen bonding (e.g., TFE, 1,1,1,3,3,3-hexafluoroisopropanol (HFIP), formic acid, and trifluoroacetic acid) can dissolve polysulfobetaines among organic solvents, it was assumed to cause no detrimental effect upon the whole step. The conversion of PGLBT calculated by monomer signals (5.7–6.2 ppm, from vinyl ends) with polymer peaks or PETTC peaks (7.4 ppm, from phenyl group) was 90% at 1 h and reached virtually full conversion (~99%) at 3 h. The disappearance of monomer peaks by reaction time is shown in Fig. 1a. SPE monomer, additional initiator, and water for the second step were subsequently transferred into the quenched PGLBT solution. Only water was added as an additional solvent because of increased hydrophilicity of the CTA after PGLBT growth. The monomer concentration ([SPE]) was kept lower than GLBT at the first step to prevent inhomogeneous mixing. On the second block synthesis, an aliquot withdrawn at 2 h showed no clearly visible monomer peaks, and the reaction was terminated at 3 h. The ^{1}H NMR spectra of the crude product as shown in Fig. 1b shows additional peaks of SPE repeating units in comparison with the signals of $GLBT_{49}$. The molecular weight distribution (MWD) (Fig. 1c) of the diblock copolymers showed a clear shift from a low (homopolymer) to higher molecular weight without residues, suggesting that almost every PGLBT macroCTA participated in the SPE

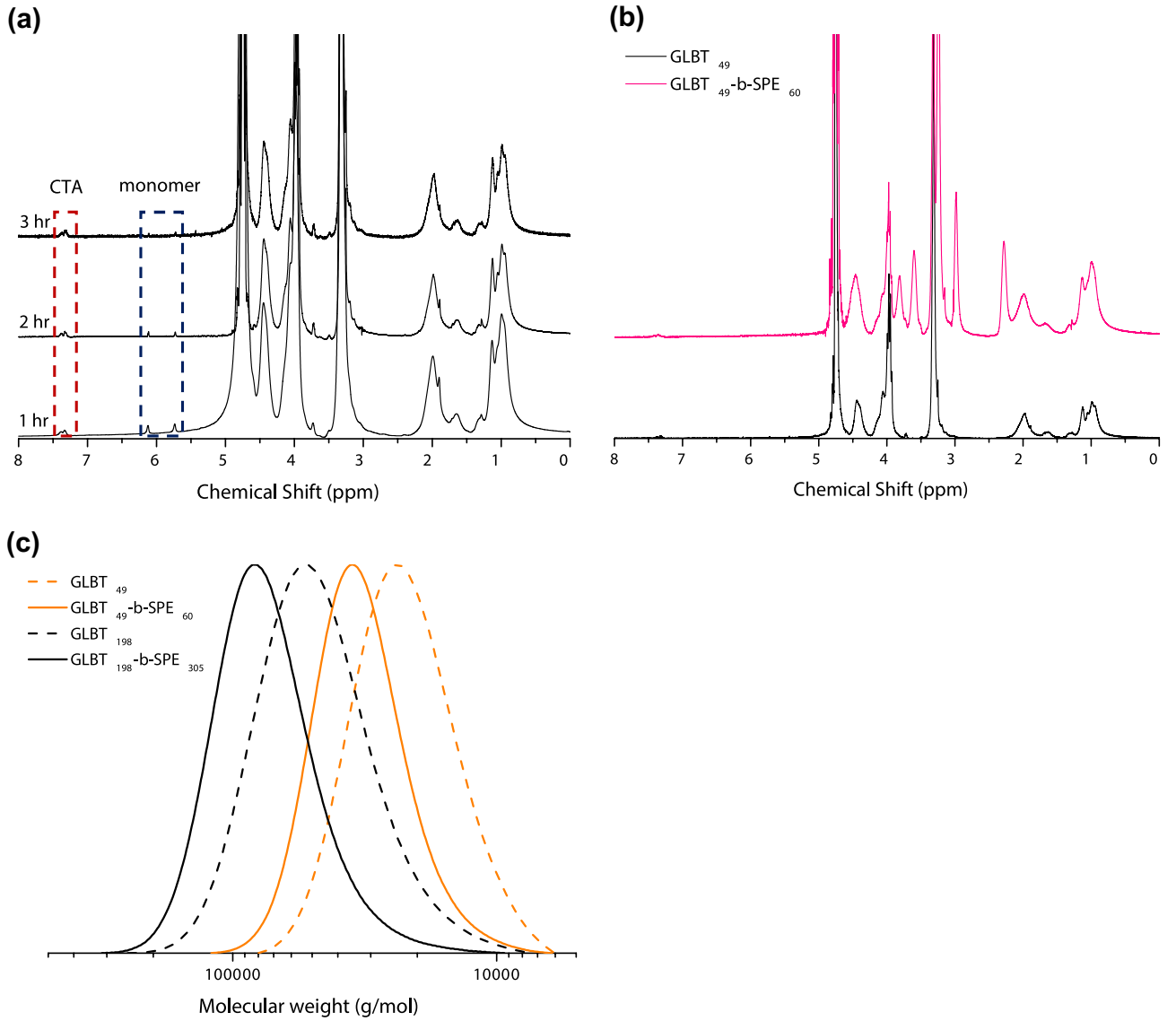

Fig. 1 **a** ^{1}H NMR spectra of $GLBT_{49}$ taken at 1 h intervals. **b** ^{1}H NMR spectra of $GLBT_{49}$ (black) and $GLBT_{49}$-*b*-SPE_{60} (red) obtained from aliquots withdrawn after 3 h. **c** MWDs of $GLBT_{49}$ and $GLBT_{49}$-*b*-SPE_{60}, and $GLBT_{198}$ and $GLBT_{198}$-*b*-SPE_{305} by SEC analysis

Table 1 Summary of the betaine block copolymers synthesized in the study

Obtained polymers[a)]	$M_{n\ theo}$ (g/mol)	$M_{n\ SEC}$[b)] (g/mol)	$Đ$ (M_w/M_n)	% L_{final}[c)]
$GLBT_{49}$-*b*-SPE_{60}	27,600	25,700	1.14	91
$GLBT_{99}$-*b*-SPE_{121}	55,500	31,200	1.12	91
$GLBT_{198}$-*b*-SPE_{305}	128,000	68,300	1.21	87
MPC_{198}-*b*-SPE_{205}	116,100	71,400	1.29	87
SPE_{49}-*b*-$GLBT_{46}$-*b*-SPE_{55}	39,300	40,100	1.16	83
SPE_{99}-*b*-$GLBT_{193}$-*b*-SPE_{135}	107,300	71,000	1.33	79

[a)]The DP values were determined by ^{1}H NMR analysis

[b)]Determined by SEC with a RI detector in a buffer solution (0.5 M CH_3COOH and 0.3 M of Na_2SO_4) with P2VP as molecular weight standards

[c)]$\%L_{final}$ is the percentage of the theoretically estimated portion of living chains

polymerization and formed PGLBT-*b*-PSPE. Table 1 shows the determined molecular weight and dispersity of synthesized polybetaine block copolymers, respectively.

To obtain higher molecular weight copolymers, the total DP was doubled or quadrupled with the fixed monomer feed ratio 1:1. The target DP of each segment was set to 100 and 200 with the same [CTA]/[I]. For the batch of DP_{target} = 200:200, [I] was increased twice to speed up the second polymerization step because of the reduced monomer concentration for adjusting workable viscosity. Both products resulted in relatively narrow MWD (~ 1.3) and monomodal peaks in SEC analysis. However, low molecular weight tailing was observed on the DP_{target} = 200:200 sample, which may be attributed to inhomogeneous mixing caused by viscosity increase. The DP determined by ^{1}H NMR analysis ($GLBT_{198}$-*b*-SPE_{305}) showed an excess number of SPE unit that implies an inhomogeneous solution state during the reaction. The dispersity and number imbalance were improved on the batch of DP_{target} = 100:100, in which the polymerization was carried out keeping the same [CTA]/[I] due to less viscosity increase.

PMPC-*b*-PSPE, which had a phosphobetaine instead of a carboxybetaine, was synthesized by the same method. MPC was rapidly consumed (98% after 1 h) like GLBT under the same reaction condition, and the reaction was stopped at 3 h when the olefinic proton signals of the monomer disappeared. The macroCTA PMPC subsequently reacted with SPE monomers without any purification, and yielded PMPC-*b*-PSPE after 3 h with ~ 99% conversion. The ^{1}H NMR spectra of both are shown in Fig. 2a, and the DP was estimated as 198:205. Although the relatively broad MWD ($Đ$ = 1.29) is thought to be attributed to insufficient mechanical strength while mixing the reaction solution, especially at the second step operated under an extremely viscous state, no unreacted homopolymer peak was found in the SEC trace (Fig. 2b). This indicated that most of the homo-PMPC chains conducted SPE growth.

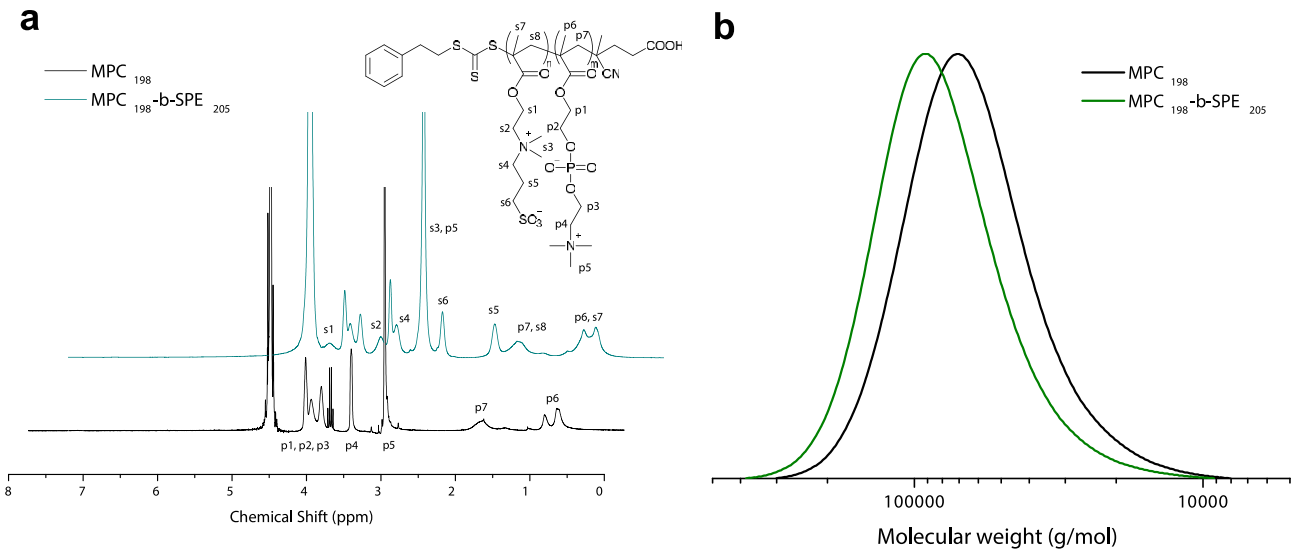

Fig. 2 **a** ^{1}H NMR spectra of MPC_{198} (black) and MPC_{198}-*b*-SPE_{205} (green). **b** MWDs of MPC_{200} (black) and MPC_{198}-*b*-SPE_{205} (green) by SEC analysis

Temperature-responsive solution behavior of obtained betaine diblock copolymers

The temperature sensitivity of three PGLBT-*b*-PSPEs targeted to have an identical PGLBT:PSPE ratio with different total DP in aqueous solution was characterized. Since PSPE segments could lose hydrophilicity below critical temperatures where intra/interchain electrostatic attractions become prominent, the PSPE moieties merge together and create an aggregate core while temperature-independent PGLBT motifs form outer layers. The hydrodynamic radii (R_h) of self-assembled core–shell particles were approximately 40–60 nm with a relatively narrow size distribution [37], which is a remarkable feature in comparison with similar polysulfobetaine-based block copolymers having a non-ionic counterpart. For example, PEG [31] or PDMAEMA [33] motifs on the opposite side of polysulfobetaine chains led to larger particles over several hundred nanometers. Dual charges of PGLBT may provide adequate repulsive force which could lead to monodisperse and relatively small-sized particle formation and prevent further agglomeration.

In this study, the three obtained PGLBT-*b*-PSPEs showed subtle variations of the transmittance and R_h compared to our previous study that showed a drastic change of size and turbidity around 20–40 °C [37]. As shown in Fig. 3a, $GLBT_{49}$-*b*-SPE_{60} existed as individual polymer chains within most of the temperature range while over 90% of the transmittance was maintained. A slow diffusive mode (mode B, the intensity-based weight was 70% at 90°) started to appear with fast-diffusing unimers (mode A) under 10 °C. The presence of the slow diffusive mode related to attractions among dipoles of the pendent groups is not only a common feature of homo-polysulfobetaine aqueous solution [5, 8] but also a prior change before monodispersed particle formation of PGLBT-*b*-PSPE as revealed in our previous study. However, monodisperse particles were not found at the end of the observation range. In accordance with Gibbs-free energy of mixing $\Delta G_m = \Delta H_m - T\Delta S_m$, the enthalpy of

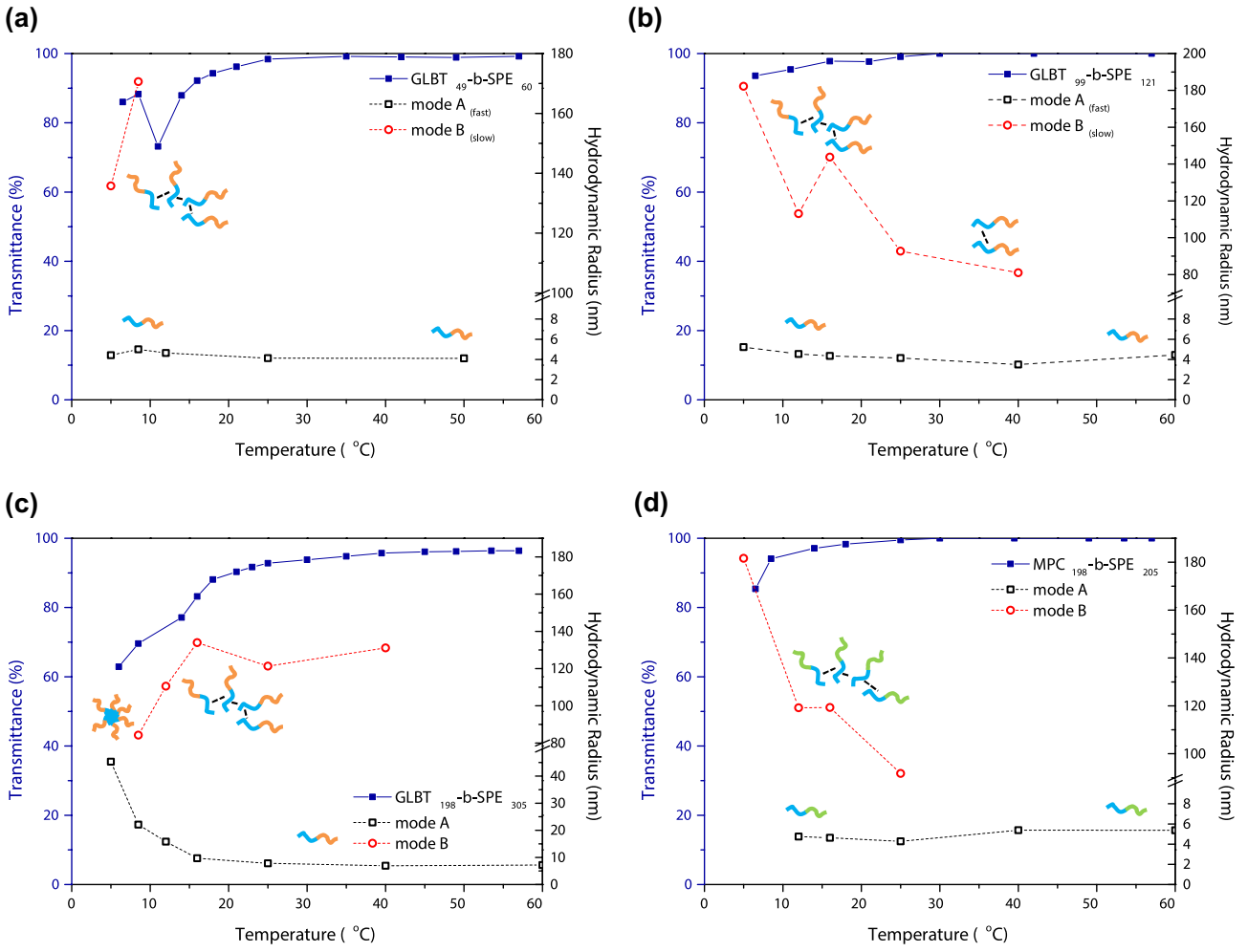

Fig. 3 Transmittance shift (left *y*-axis, solid symbols) and hydrodynamic radius variation (right *y*-axis, open symbols) by temperature of double betaine block copolymers **a** $GLBT_{49}$-*b*-SPE_{60}, **b** $GLBT_{99}$-*b*-SPE_{121}, **c** $GLBT_{198}$-*b*-SPE_{305}, and **d** MPC_{198}-*b*-SPE_{205}

mixing of the polymer may be lowered by equally numbered PGLBT to PSPE, and would become sufficient to prevent phase transition. Instead of forming self-assembled structures, the uniformly swollen and hydrated chain state is thought to be thermodynamically preferred at lower temperatures. This weak temperature-responsive solution behavior reappeared similarly on two other PGLBT-*b*-PSPEs having higher molecular weights. $GLBT_{99}$-*b*-SPE_{121} existed as unimers accompanying a size-increasing slow mode by cooling below 40 °C, and did not create monodisperse micelles (Fig. 3b). On the other hand, $GLBT_{198}$-*b*-SPE_{305} showed a significant size increase to 45 nm at the low temperature (Fig. 3c) with more visible transmittance decrease. Only the ACFs of $GLBT_{198}$-*b*-SPE_{305} showed a shift from a fast monomodal decay to a slow monomodal decay while the others were represented by broadly decaying curves at 5 °C (Fig. S1). It is thought that a higher DP imbalance of the two repeating units drives the polymer chain to create compactly packed PSPE cores below a certain temperature, whereas the nearly identical DP ratio tends to prohibit the transition and keep a polydisperse and intermediate state.

In addition, MPC_{198}-*b*-SPE_{205} showed the same behavior against temperature as the PGLBT-*b*-PSPEs did (Fig. 3d). Having almost the same DP of both respective units, the chains existed as homogeneous unimers until 25 °C, then a slow diffusive mode emerged and became dominant at the end. However, alteration to monodisperse micelles did not occur like the previous samples ($GLBT_{49}$-*b*-SPE_{60} and $GLBT_{99}$-*b*-SPE_{121}). No specific difference from PGLBT-*b*-PSPEs was found. (The ACFs and the analysis result of the MPC_{198}-*b*-SPE_{205} solution are shown in Fig. S2.) Thus, it is thought that PMPC motifs played the same role as PGLBT in PGLBT-*b*-PSPEs intervening the pairing of polysulfobetaine moieties. Polyphosphobetaines including PMPC are known to be non-responsive to temperature as polycarboxybetaines, but multiple diffusive modes in aqueous solution have been reported on double polyphosphobetaine block copolymers consisting of PMPC and inverted phosphobetaine-repeating units having slightly higher hydrophobicity [7]. Therefore, dipole–dipole attractions between PMPC and PSPE as well as PGLBT with PSPE motifs might occur, but it does not seem to be preferred and maintained firmly than the pairing among PSPE moieties, which create cores of monodisperse micelles.

One-pot polymerization of triblock betaine copolymers

The arrangement of betaine block copolymers was extended to three consecutive polymerizations through the one-pot approach. In the experiment, PSPE was synthesized prior to PGLBT then thirdly for yielding double PSPE-ended chains, which were expected to show additional possible interaction modes, so that more complex temperature-responsive behaviors than that of diblock copolymers may be envisaged. Each batch was aimed to synthesize 50 units ($DP_{target} = 50$), and the monomer concentration [M] and [CTA]/[I] was not modified from the condition of the diblock copolymer synthesis except the third step in which [M] was reduced to 1 M to prevent inhomogeneous mixing due to extreme increase in viscosity. A larger amount of initiator (twice the usual) was added to maintain the reaction speed similarly. On the first step, SPE was quickly consumed and the conversion reached ~ 100% at 3 h as confirmed from ^{1}H NMR signals of aliquots. The second and third blocks were successively synthesized allowing 3 h for each process with no visible monomer peaks found in ^{1}H NMR spectra. Each block was represented by increasing proton signals of the respective functional groups as shown in Fig. 4a, and the DP was determined to be 49:46:55 from the integral ratio. The MWDs (Fig. 4b) of aliquots showed a clear shift to a higher molecular weight region without any shoulders, which revealed full conversion at each step. Since the cumulative chain livingness at the second step was calculated to be 91%, slight tailing of the SEC trace on the final product indicating "dead chain" was inevitable. In spite of the relatively low chain livingness, MWD was kept at about 1.2. Another triblock of the same sequence was aimed to obtain DP as 100:200:100 for SPE/GLBT/SPE, and it was determined as 99:193:135 by the integral ratio.

Temperature-responsive solution behavior of PSPE-*b*-PGLBT-*b*-PSPE triblock copolymers

The solution behavior of triblocks PSPE-*b*-PGLBT-*b*-PSPE was elucidated by turbidimetry and DLS. The first triblock sample (SPE_{49}-*b*-$GLBT_{46}$-*b*-SPE_{55}) had DPs almost identical with those of the three blocks so that the portion of PSPE was twice that of PGLBT. As a result, the aqueous solution showed more noticeable transmittance and size change (displayed in Fig. 5a and c) than the previously examined diblock copolymer samples that had an almost identical DP ratio. Alongside a fast diffusive mode representing freely moving polymer chains, a slow mode emerged below ~ 40 °C while the transmittance gradually decreased, and persistently appeared until 12 °C where the transmittance started decreasing substantially up to 0%. The slow diffusive mode eventually disappeared and uniformly size-distributed particles appeared as diblock copolymer solutions. The slow diffusive large components were not predominant up to 25 °C (Fig. 5c) and the intensity-based weight increased to 57% at 17 °C and 97% at 12 °C (intensity-based weight at scattering angle = 90°). The slow mode in the intermediate region is assumed to be aggregated chain clusters originating from dipole–dipole interaction, especially among PSPE segments on both ends of a chain. Its size varied largely

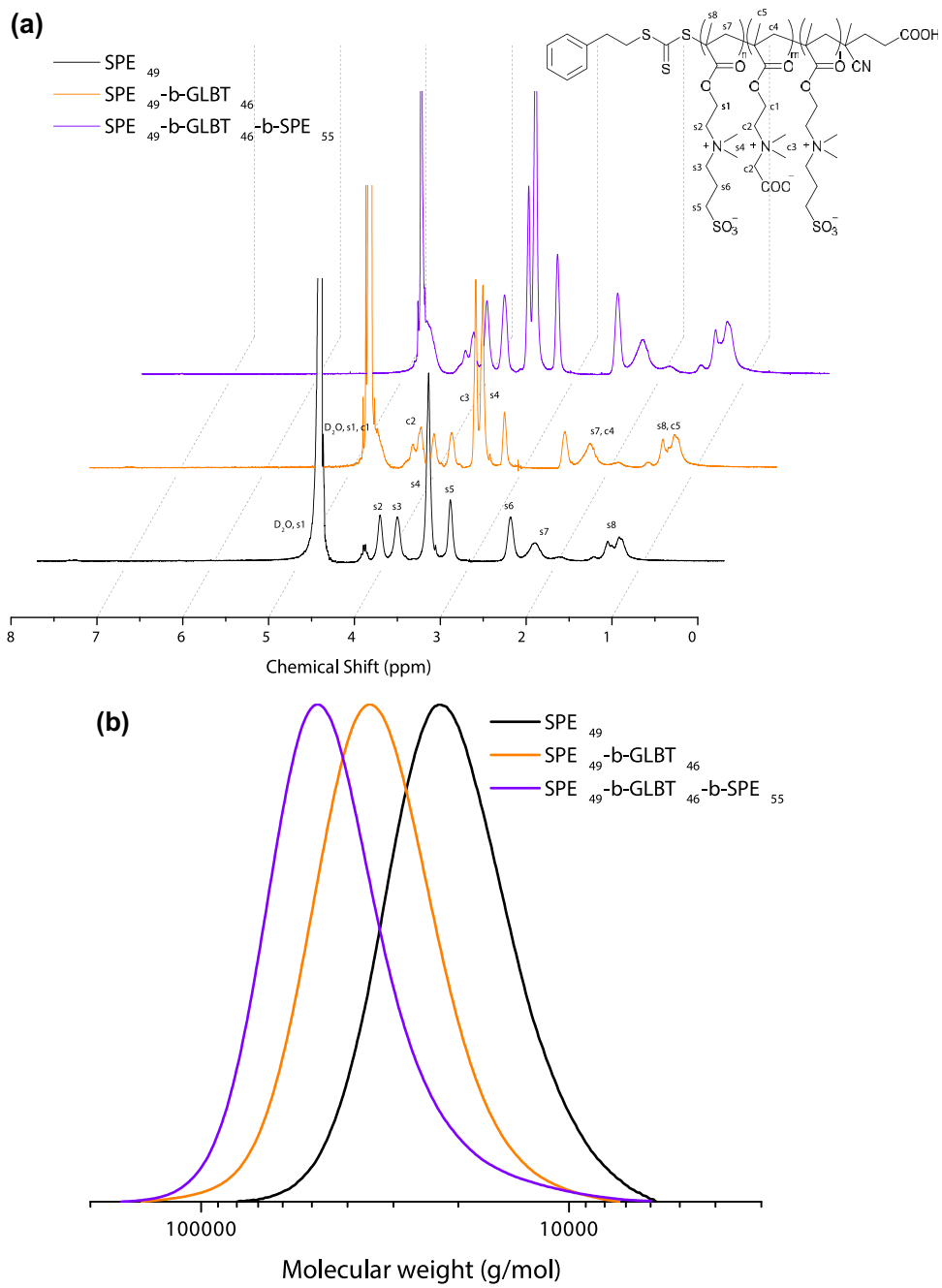

Fig. 4 **a** ^{1}H NMR spectra (obtained at 60 °C) of SPE_{49}-*b*-$GLBT_{46}$-*b*-SPE_{55} on each synthesis step. **b** MWDs by SEC analysis of SPE_{49}-*b*-$GLBT_{46}$-*b*-SPE_{55}

from R_h = ~200 nm to 700 nm, and the decay rates of two modes were linear with q^2 for all scattering angles, which represents translational diffusion of objects. (An example at 25 °C is shown in Fig. S3.) Since temperature-independent PGLBT motifs were placed between both PSPE sides, the monodisperse particles (R_h = ~30 nm, PDI ($\mu_2/\overline{\Gamma}^2$) = 0.12 by cumulant fit) at 5 °C are assumed as "flower" micelles consisting of PGLBT loops and PSPE cores.

On the other hand, the thermoresponsive behavior of the SPE_{99}-*b*-$GLBT_{193}$-*b*-SPE_{135} solution pronounced at lower temperatures, which might be attributed to the lower PSPE-PGLBT. The transmittance was kept over 90% with some extent of a slow mode. (R_h = ~130 nm, intensity-based weight = 17% at 40 °C and 76% at 25 °C at scattering angle = 90°) Then, a rapid transmittance shift occurred with size variation at around 20 °C and the polydisperse state turned into the fairly monodisperse state around 16 °C (Fig. S3(c)). Under 16 °C, a single diffusive mode was determined as a larger R_h than that of the previous triblock sample, and the size gradually reduced with the decrease in temperature. (R_h = 132 nm, PDI ($\mu_2/\overline{\Gamma}^2$) = 0.22, 5 °C) For reconfirmation of the temperature-responsive behavior of

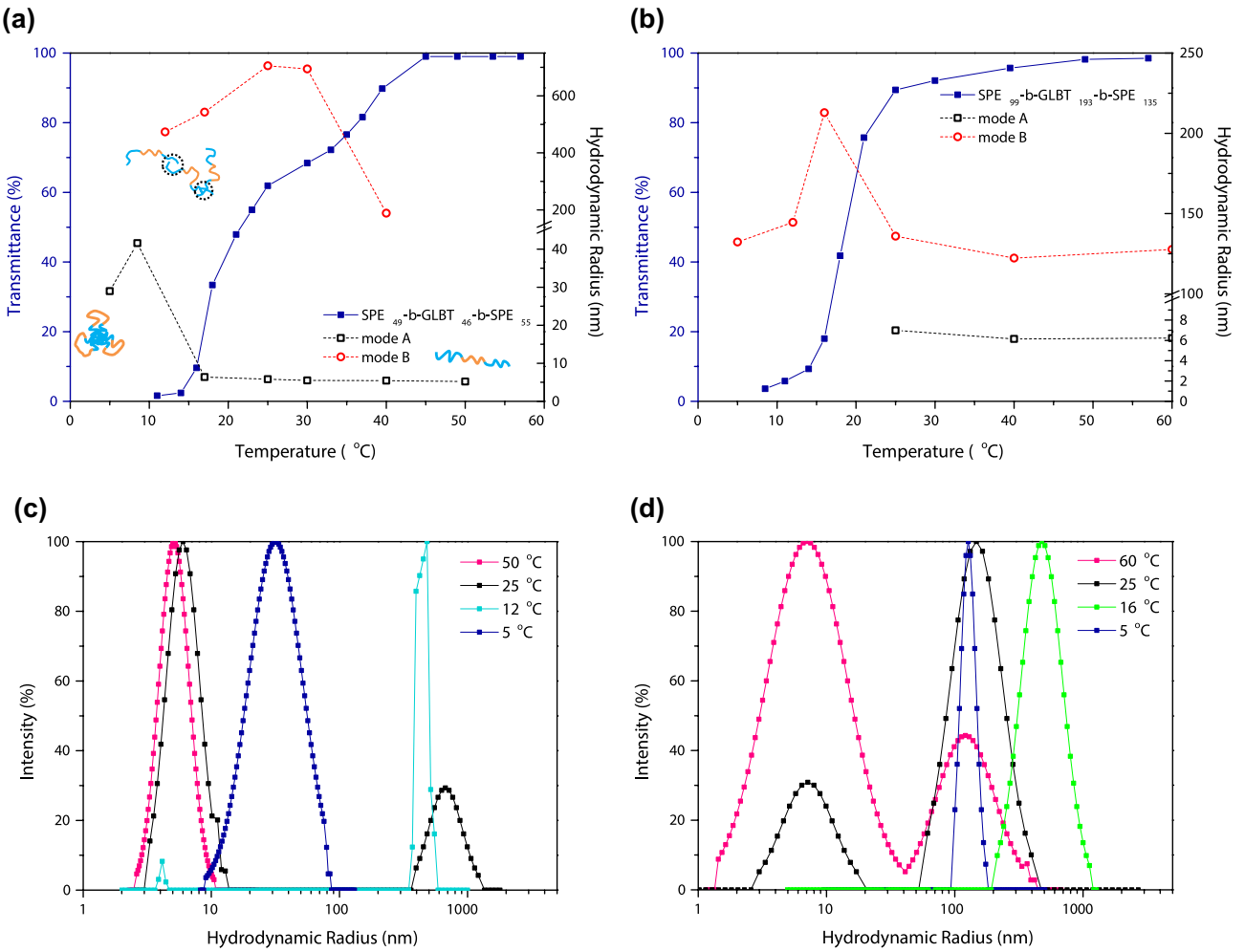

Fig. 5 Transmittance shift (left *y*-axis, solid symbols) and hydrodynamic radius variation (right *y*-axis, open symbols) of triblock betaine copolymers against temperatures **a** SPE_{49}-*b*-$GLBT_{46}$-*b*-SPE_{57} and **b** SPE_{99}-*b*-$GLBT_{193}$-*b*-SPE_{135} (The ACFs collected at each temperature are separately shown in Fig. S3.) Intensity-based distribution of hydrodynamic radii at various temperatures (**c**) SPE_{49}-*b*-$GLBT_{46}$-*b*-SPE_{57} (**d**) SPE_{99}-*b*-$GLBT_{193}$-*b*-SPE_{135}

the triblock, we synthesized an extra triblock copolymer with the same target DP in each block, and it was characterized as SPE_{100}-*b*-$GLBT_{198}$-*b*-SPE_{104} by ^{1}H NMR analysis. ($M_n^{SEC} = 48{,}100$ g/mol, $Đ = 1.12$) However, the triblock copolymer whose block ratio was more precisely controlled showed weaker responses to temperature as the diblock copolymers having a ratio close to 1:1 (the results are shown in Fig. S4). The dual diffusive mode state continued to 5 °C with over 90% transmittance, and the transition to a single diffusive mode state did not occur. Accordingly, the difference in total unit number of respective PGLBT and PSPE may affect the chain behavior crucially, whether it is AB-type diblock or BAB-type triblock.

Conclusion

We synthesized betaine block copolymers PGLBT-*b*-PSPE and PMPC-*b*-PSPE by one-pot RAFT polymerization and investigated their temperature-responsive properties in aqueous solution. The concentrations of monomers and initiator were carefully optimized to achieve full conversion of betaine methacrylate monomers with DPs of more than 50 within 3 h at 70 °C. By utilizing a trithiocarbonate RAFT agent with minimum usage of the radical initiator in water, full consumption of the betaine monomers was achieved and no purification after the first polymerization step was required. This method enabled to get well-defined betaine triblock

copolymers through reduced time and simplified purification compare to the previous RAFT or ATRP-mediated two-step synthesis [41]. The activity of macroCTA corresponded to the theoretically estimated chain livingness in contrast to our previous study [37], in which the macroCTAs had lost the chain livingness significantly. In order to keep accessible viscosity and high DP, a larger amount of initiator was used at a relatively low monomer concentration and this led to a lower chain livingness after the second step (~ 90%) in comparison to the original one-pot RAFT multiblock synthesis method [44]. Nevertheless, betaine diblocks and triblocks could be prepared with narrow MWD (~ 1.3) and aimed block ratios. The three PGLBT-*b*-PSPE having different total DP but nearly equal block ratio commonly showed little behavior change with temperature. Unimers with some extent of slow diffusive objects thought to loosely aggregated chain clusters existed over a wide temperature range while the solutions were highly transparent, and the percentage of aggregates increased with decreasing temperature. However, only a sample holding apparently more SPE units than GLBT assembled polymer micelles as demonstrated in our previous study. Two BAB-type triblocks that consisted of both PSPE ends showed a more noticeable behavior change dependent on the entire ratio of PGLBT:PSPE. The triblock with a 1:1:1 ratio showed a clear macroscopic change in water while both ends of PSPE induced larger aggregates under a gradual transmittance decrease. The chains formed monodisperse particles below 10 °C, which is assumed to be "flower" micelles. More detailed studies on the influence of block ratio and chain length on the temperature-responsive behavior of PGLBT-*b*-PSPE are underway.

Supplementary Information The online version contains supplementary material available at https://doi.org/10.1007/s00396-021-04846-1.

Data availability Data are available on request from the authors.

Declarations

Conflict of interest The authors declare no competing interests.

References

1. Laschewsky A, Rosenhahn A (2019) Molecular design of zwitterionic polymer interfaces: Searching for the difference. Langmuir 35(5):1056–1071. https://doi.org/10.1021/acs.langmuir.8b01789
2. Georgiev GS, Karnenska EB, Vassileva ED, Kamenova IP, Georgieva VT, Iliev SB, Ivanov IA (2006) Self-assembly, anti polyelectrolyte effect, and nonbiofouling properties of polyzwitterions. Biomacromol 7(4):1329–1334. https://doi.org/10.1021/bm050938q
3. Mary P, Bendejacq DD, Labeau MP, Dupuis P (2007) Reconciling low- and high-salt solution behavior of sulfobetaine polyzwitterions. J Phys Chem B 111(27):7767–7777. https://doi.org/10.1021/jp071995b
4. Hildebrand V, Laschewsky A, Pach M, Muller-Buschbaum P, Papadakis CM (2017) Effect of the zwitterion structure on the thermo-responsive behaviour of poly(sulfobetaine methacrylates). Polym Chem 8(1):310–322. https://doi.org/10.1039/c6py01220e
5. Cao ZL, Zhang GZ (2015) Dynamics of polyzwitterions in salt-free and salt solutions. Phys Chem Chem Phys 17(40):27045–27051. https://doi.org/10.1039/c5cp04827c
6. Niu AZ, Liaw DJ, Sang HC, Wu C (2000) Light-scattering study of a zwitterionic polycarboxybetaine in aqueous solution. Macromolecules 33(9):3492–3494. https://doi.org/10.1021/ma991622b
7. Morozova S, Hu G, Emrick T, Muthukumar M (2016) Influence of dipole orientation on solution properties of polyzwitterions. ACS Macro Lett 5(1):118–122. https://doi.org/10.1021/acsmacrolett.5b00876
8. Delgado JD, Schlenoff JB (2017) Static and dynamic solution behavior of a polyzwitterion using a Hofmeister salt series. Macromolecules 50(11):4454–4464. https://doi.org/10.1021/acs.macromo1.7b00525
9. Forster S, Schmidt M, Antonietti M (1990) Static and dynamic light-scattering by aqueous polyelectrolyte solutions - effect of molecular-weight. charge-density and added salt Polymer 31(5):781–792. https://doi.org/10.1016/0032-3861(90)90036-x
10. Schmidt M (1989) Static and dynamic light-scattering by an aqueous poly-electrolyte solution without added salt - quaternized poly(2-vinylpyridine). Makromolekulare Chemie-Rapid Communications 10(2):89–96
11. Jia D, Muthukumar M (2019) Effect of salt on the ordinary-extraordinary transition in solutions of charged macromolecules. J Am Chem Soc 141(14):5886–5896. https://doi.org/10.1021/jacs.9b00562
12. Kitano H, Sudo K, Ichikawa K, Ide M, Ishihara K (2000) Raman spectroscopic study on the structure of water in aqueous polyelectrolyte solutions. J Phys Chem B 104(47):11425–11429. https://doi.org/10.1021/jp000429c
13. Kitano H, Imai M, Sudo K, Ide M (2002) Hydrogen-bonded network structure of water in aqueous solution of sulfobetaine polymers. J Phys Chem B 106(43):11391–11396. https://doi.org/10.1021/jp020185r
14. Leng C, Hung HC, Sun SW, Wang DY, Li YT, Jiang SY, Chen Z (2015) Probing the surface hydration of nonfouling zwitterionic and PEG materials in contact with proteins. ACS Appl Mater Interfaces 7(30):16881–16888. https://doi.org/10.1021/acsami.5b05627
15. Leng C, Sun SW, Zhang KX, Jiang SY, Chen Z (2016) Molecular level studies on interfacial hydration of zwitterionic and other antifouling polymers in situ. Acta Biomater 40:6–15. https://doi.org/10.1016/j.actbio.2016.02.030
16. Schlenoff JB (2014) Zwitteration: coating surfaces with zwitterionic functionality to reduce nonspecific adsorption. Langmuir 30(32):9625–9636. https://doi.org/10.1021/la500057j
17. Ladd J, Zhang Z, Chen S, Hower JC, Jiang S (2008) Zwitterionic polymers exhibiting high resistance to nonspecific protein adsorption from human serum and plasma. Biomacromol 9(5):1357–1361. https://doi.org/10.1021/bm701301s
18. Guo SS, Janczewski D, Zhu XY, Quintana R, He T, Neoh KG (2015) Surface charge control for zwitterionic polymer brushes: tailoring surface properties to antifouling applications. J Colloid Interface Sci 452:43–53. https://doi.org/10.1016/j.jcis.2015.04.013
19. Woodfield PA, Zhu YC, Pei YW, Roth PJ (2014) Hydrophobically modified sulfobetaine copolymers with tunable aqueous UCST through postpolymerization modification of poly(pentafluorophenyl acrylate). Macromolecules 47(2):750–762. https://doi.org/10.1021/ma402391a
20. Chang Y, Liao SC, Higuchi A, Ruaan RC, Chu CW, Chen WY (2008) A Highly stable nonbiofouling surface with well-packed grafted zwitterionic polysulfobetaine for plasma protein

repulsion. Langmuir 24(10):5453–5458. https://doi.org/10.1021/la800228c
21. Das M, Sanson N, Kumacheva E (2008) Zwitterionic poly(betaine-N-isopropylacrylamide) microgels: properties and applications. Chem Mater 20(22):7157–7163. https://doi.org/10.1021/cm801585x
22. Zhao Y, Bai T, Shao Q, Jiang SY, Shen AQ (2015) Thermoresponsive self-assembled NiPAm-zwitterion copolymers. Polym Chem 6(7):1066–1077. https://doi.org/10.1039/c4py01553c
23. Fevola MJ, Bridges JK, Kellum MG, Hester RD, McCormick CL (2004) pH-responsive polyzwitterions: a comparative study of acrylamide-based polyampholyte terpolymers and polybetaine copolymers. J Appl Polym Sci 94(1):24–39. https://doi.org/10.1002/app.20700
24. Kathmann EEL, White LA, McCormick CL (1997) Water-soluble polymers .73. Electrolyte- and pH-responsive zwitterionic copolymers of 4- (2-acrylamido-2-methylpropyl)dimethylammonio butanoate with 3- (2-acrylamido-2-methylpropyl)dimethylammonio propanesulfonate. Macromolecules 30 (18):5297–5304. https://doi.org/10.1021/ma961214x
25. Danko M, Kronekova Z, Mrlik M, Osickabin Yousaf A, Mihalova A, Tkac J, Kasak P, J (2019) Sulfobetaines meet carboxybetaines: modulation of thermo- and ion-responsivity, water structure, mechanical properties, and cell adhesion. Langmuir 35(5):1391–1403. https://doi.org/10.1021/acs.langmuir.8b01592
26. Matsuoka H, Yamakawa Y, Ghosh A, Saruwatari Y (2015) Nanostructure and salt effect of zwitterionic carboxybetaine brush at the air/water interface. Langmuir 31(17):4827–4836. https://doi.org/10.1021/acs.langmuir.5b00637
27. Murugaboopathy S, Matsuoka H (2015) Salt-dependent surface activity and micellization behaviour of zwitterionic amphiphilic diblock copolymers having carboxybetaine. Colloid Polym Sci 293(5):1317–1328. https://doi.org/10.1007/s00396-015-3503-1
28. Doncom KEB, Warren NJ, Armes SP (2015) Polysulfobetaine-based diblock copolymer nano-objects via polymerization-induced self-assembly. Polym Chem 6(41):7264–7273. https://doi.org/10.1039/c5py00396b
29. Doncom KEB, Willcock H, O'Reilly RK (2017) The direct synthesis of sulfobetaine-containing amphiphilic block copolymers and their self-assembly behavior. Eur Polymer J 87:497–507. https://doi.org/10.1016/j.eurpolymj.2016.09.002
30. Mai T, Boye S, Yuan J, Volkel A, Grawert M, Gunter C, Lederer A, Taubert A (2015) Poly(ethylene oxide)-based block copolymers with very high molecular weights for biomimetic calcium phosphate mineralization. RSC Adv 5(125):103494–103505. https://doi.org/10.1039/c5ra20035k
31. Nizardo NM, Schanzenbach D, Schonemann E, Laschewsky A (2018) Exploring Poly(ethylene glycol)-Polyzwitterion Diblock Copolymers as Biocompatible Smart Macrosurfactants Featuring UCST-Phase Behavior in Normal Saline Solution. Polymers 10 (3). https://doi.org/10.3390/polym10030325
32. Wang D, Wu T, Wan XJ, Wang XF, Liu SY (2007) Purely salt-responsive micelle formation and inversion based on a novel schizophrenic sulfobetaine block copolymer: Structure and kinetics of micellization. Langmuir 23(23):11866–11874. https://doi.org/10.1021/la702029a
33. Sun H, Chen XL, Han X, Liu HL (2017) Dual thermoresponsive aggregation of schizophrenic PDMAEMA-b-PSBMA copolymer with an unrepeatable pH response and a recycled CO2/N-2 response. Langmuir 33(10):2646–2654. https://doi.org/10.1021/acs.langmuir.7b00065
34. Vishnevetskaya NS, Hildebrand V, Niebuur BJ, Grillo I, Filippov SK, Laschewsky A, Muller-Buschbaum P, Papadakis CM (2017) "Schizophrenic" micelles from doubly thermoresponsive polysulfobetaine-b-poly(N-isopropylmethacrylamide) diblock copolymers. Macromolecules 50(10):3985–3999. https://doi.org/10.1021/acs.macromol.7b00356
35. Vishnevetskaya NS, Hildebrand V, Dyakonova MA, Niebuur BJ, Kyriakos K, Raftopoulos KN, Di ZY, Muller-Buschbaum P, Laschewsky A, Papadakis CM (2018) Dual orthogonal switching of the "schizophrenic" self-assembly of diblock copolymers. Macromolecules 51(7):2604–2614. https://doi.org/10.1021/acs.macromol.8b00096
36. Hippius C, Butun V, Erel-Goktepe I (2014) Bacterial anti-adhesive properties of a monolayer of zwitterionic block copolymer micelles. Materials Science & Engineering C-Materials for Biological Applications 41:354–362. https://doi.org/10.1016/j.msec.2014.04.023
37. Lim J, Matsuoka H, Yusa S, Saruwatari Y (2019) Temperature-responsive behavior of double hydrophilic carboxy-sulfobetaine block copolymers and their self-assemblies in water. Langmuir 35(5):1571–1582. https://doi.org/10.1021/acs.langmuir.8b02952
38. Lim J, Matsuoka H, Saruwatari Y (2020) Effects of pH on the stimuli-responsive characteristics of double betaine hydrophilic block copolymer PGLBT-b-PSPE. Langmuir 36(7):1727–1736. https://doi.org/10.1021/acs.langmuir.9b03682
39. Lim J, Matsuoka H, Saruwatari Y (2020) Effects of halide anions on the solution behavior of double hydrophilic carboxy-sulfobetaine block copolymers. Langmuir 36(19):5165–5175. https://doi.org/10.1021/acs.langmuir.0c00325
40. Takahashi M, Shimizu A, Yusa SI, Higaki Y (2021) Lyotropic morphology transition of double zwitterionic diblock copolymer aqueous solutions. Macromolecular Chemistry and Physics 222 (4). https://doi.org/10.1002/macp.202000377
41. Taylor ME, Lounder SJ, Asatekin A, Panzer MJ (2020) Synthesis and self-assembly of fully zwitterionic triblock copolymers. Acs Materials Letters 2(3):261–265. https://doi.org/10.1021/acsmaterialslett.9b00500
42. G Gody T Maschmeyer PB Zetterlund S Perrier 2013 Rapid and quantitative one-pot synthesis of sequence-controlled polymers by radical polymerization Nat Commun 4 https://doi.org/10.1038/ncomms3505
43. Gody G, Maschmeyer T, Zetterlund PB, Perrier S (2014) Exploitation of the degenerative transfer mechanism in RAFT polymerization for synthesis of polymer of high livingness at full monomer conversion. Macromolecules 47(2):639–649. https://doi.org/10.1021/ma402286e
44. Gody G, Maschmeyer T, Zetterlund PB, Perrier S (2014) Pushing the limit of the RAFT process: multiblock copolymers by one-pot rapid multiple chain extensions at full monomer conversion. Macromolecules 47(10):3451–3460. https://doi.org/10.1021/ma402435n
45. Gody G, Barbey R, Danial M, Perrier S (2015) Ultrafast RAFT polymerization: multiblock copolymers within minutes. Polym Chem 6(9):1502–1511. https://doi.org/10.1039/c4py01251h
46. Martin L, Gody G, Perrier S (2015) Preparation of complex multiblock copolymers via aqueous RAFT polymerization at room temperature. Polym Chem 6(27):4875–4886. https://doi.org/10.1039/c5py00478k
47. Jones ER, Semsarilar M, Blanazs A, Armes SP (2012) Efficient synthesis of amine-functional diblock copolymer nanoparticles via RAFT dispersion polymerization of benzyl methacrylate in alcoholic media. Macromolecules 45(12):5091–5098. https://doi.org/10.1021/ma300898e
48. Baussard JF, Habib-Jiwan JL, Laschewsky A, Mertoglu M, Storsberg J (2004) New chain transfer agents for reversible addition-fragmentation chain transfer (RAFT) polymerisation in aqueous solution. Polymer 45(11):3615–3626. https://doi.org/10.1016/j.polymer.2004.03.081
49. Fuchs AV, Thurecht KJ (2017) Stability of trithiocarbonate RAFT agents containing both a cyano and a carboxylic acid functional group. ACS Macro Lett 6(3):287–291. https://doi.org/10.1021/acsmacrolett.7b00100
50. Moad G (2014) Mechanism and kinetics of dithiobenzoate-mediated RAFT polymerization - status of the dilemma. Macromol Chem Phys 215(1):9–26. https://doi.org/10.1002/macp.201300562

51. Williams M, Penfold NJW, Lovett JR, Warren NJ, Douglas CWI, Doroshenko N, Verstraete P, Smets J, Armes SP (2016) Bespoke cationic nano-objects via RAFT aqueous dispersion polymerisation. Polym Chem 7(23):3864–3873. https://doi.org/10.1039/c6py00696e
52. Lovett JR, Warren NJ, Ratcliffe LPD, Kocik MK, Armes SP (2015) pH-Responsive non-ionic diblock copolymers: ionization of carboxylic acid end-groups induces an order-order morphological transition. Angewandte Chemie-International Edition 54(4):1279–1283. https://doi.org/10.1002/anie.201409799
53. Penfold NJW, Lovett JR, Warren NJ, Verstraete P, Smets J, Armes SP (2016) pH-responsive non-ionic diblock copolymers: protonation of a morpholine end-group induces an order-order transition. Polym Chem 7(1):79–88. https://doi.org/10.1039/c5py01510c
54. Valdebenito A, Encinas MV (2010) Effect of solvent on the free radical polymerization of N. N-dimethylacrylamide Polymer International 59(9):1246–1251. https://doi.org/10.1002/pi.2856